



Study of gas laminar flow in a thermal reactor: Experimental and Numerical comparison

A. Bellil^{1,2}, K. Benhabib², P. Coorevits², C. Marie², M. Hazi¹, A. Ould-Driss¹

¹University of Technology of Compiègne, TIMR (EA 4297), Rue du Dr Schweitzer, Compiègne, 60200, France

²University of Picardie Jules Verne, EPROAD (EA 4669) IUT de l'Aisne, 48 Rue d'Ostende, Saint-Quentin, 02100, France

Received 16 Dec 2014, Revised 28 Feb 2015, Accepted 28 Feb 2015

*Corresponding author: E-mail : karim.benhabib@u-picardie.fr

Abstract

The energy conversion in a thermal reactor has a negative impact on the environment, due to the emission of greenhouse gases. It is also related to energy consumption, which is important for weak yields, and creates problems for reacting flows. The present contribution aims to optimize the operation of energy equipment and prevent their dysfunction. The objective of this study is the development of experimental method for the characterization of gas flows in order to determine the residence times distribution (RTD) for gaseous phases. On the other hand, developing a numerical model that combines a discrete granular behavior Discrete Element Method (DEM) and type of approach continues, Computational Fluid Dynamics (CFD) thus allowing optimization and extrapolation facilities of an industrial scale to mitigate the shortcomings observed in the reactors such as, dead zones or poor fluidization, short circuits, etc... Our first approach is based on a finite volume CFD modeling of the behavior of a single-phase fluid, this model allows us to obtain the trajectory of a particle and the residence time distribution. The experimental study performed in parallel, allows us to validate our numerical model and apply it to other configurations.

Keywords: Residence Times Distribution (RTD) ; Computational Fluid Dynamics (CFD); Discrete Element Method (DEM); Laminar flow.

1. Introduction

Technical applications of chemical reaction engineering often rely on the interaction between chemical kinetics and fluid dynamics. In chemical reactors, the interplay between both processes is often characterized in terms of the reactors residence time distribution (RTD). The differential residence time distribution is a probability density function that describes the amount of time that fluid elements spend within the reactor [1-2]. The (RTD) is of fundamental importance for estimating the yield and selectivity of any reaction in a certain reactor. Dankwerts et al. [3] have analyzed an important number of RTDs. This concept has become both a fundamental part of any book on chemical engineering and an important tool for characterization of any technical chemical reactor [4]. However, recent studies on the theory of residence time and these applications in fields are as diverse as chemistry and process engineering, chromatography, medicine, geosciences and oceanography. Today the study of (RTD) affects several areas and different networks will scale distribution of drinking water to the micro-capillary [5-7]. In classical large scale chemical reactors the fluid flow is usually turbulent and the RTD is often described by the tank-in series model or the one dimensional axial dispersion model [8]. There are two types of measuring methods of RTD; we chose the non-intrusive method, that is to say: without disruption. In the family of no-intrusive method, we discuss the method of tracing: The method consists of associating with the fluid molecules a proportion of detectable molecules. However this tracer must have the same flow properties of fluid. The technique consists of making a disturbance of concentration of the labeled molecules to the input of the system and then to follow the variations of the outlet concentration. The tracer detection can be performed optically or conductively. Mainly two kinds of optical detection systems were reported. Digital image processing and color meter were used to analyze the color of photos or the signal from the sensor directly [8]. Fluorescence analysis also belongs to this kind of detection, which was applied more in a dark environment with accurate sensors [9]. Another optical detection vastly reported in literature, utilizes different types of spectroscopy to analyze the light absorbance of the tracer, for example, Parker blue dye dissolved in water [10].

Near infrared (NIR) and ultraviolet (UV) are two commonly used regions of the spectrum, reported by many investigators [11-15] and [16] helium was used as the inert tracer in this study. Tracer using organic gas such as propane was also reported, the detection of which was using inline gas chromatography in a CFB system [17].

2.1 Theory of residence time distribution for a laminar flow regime

From the RTD, we can calculate a number of parameters describing the transit of the tracer in the system and the behavior of the fluid traced if the physical properties of the tracer and the fluid are similar. The RTD can be described by time intervals which characterizes the distribution of the tracer cloud. In pure convective transport the cumulative residence time distribution function $F(t)$ describes the fraction of fluid that leaves the reactor [9] with age less than t and is thus given by :

$$F(t) = \frac{Q(t)}{Q_{total}} \tag{1}$$

where, $Q(t)$ is the volumetric flow rate associated with a residence time t or lower and Q_{total} is the total volumetric flow rate. The differential residence time distribution function $E(t)$ is related to the cumulative residence time distribution by:

$$E(t) = \frac{dF(t)}{dt} \tag{2}$$

In this paper we consider the laminar flow of a single phase fluid (gas) in a cylindrical geometry and we are interested in the RTD from the velocity profile. For laminar flow through a circular pipe it is:

$$v(r) = v_0 \left[1 - \left(\frac{r}{R} \right)^2 \right] \tag{3}$$

where R and v_0 are respectively the radius of the pipe and the maximum velocity, which corresponds to the current line in the center of the axes of abscissas. The minimum time t_{min} is so:

$$t_{min} = \frac{L}{v_0} \tag{4}$$

where L is the distance traversed. $E(t)$ is the tracer flows normalized relative to the volume of tracer returned. It can also be written as:

$$E(t) = \frac{dQ}{Q} = \frac{2v(r)}{v_{mean}R^2} r dr \tag{5}$$

giving that $E(t) = 0$ if $t < t_{min}$ and $E(t) = 2 \frac{t_{min}^2}{t^3}$ if $t > t_{min}$ \tag{6}

With $t_{min} = \frac{2v_{mean}}{L}$ \tag{7}

Thus

$$\int_0^{\infty} E(t) dt = 1 \tag{8}$$

where Q is the flowrate of the fluid.

$$\bar{t}_s = \int_0^{\infty} tE(t) dt = \int_{t_{min}}^{\infty} \frac{2t_{min}^2}{t^2} dt = \left[-\frac{2t_{min}^2}{t} \right]_{t_{min}}^{\infty} = 2t_{min} \tag{9}$$

\bar{t}_s is the mean or average residence time.

1.2 Model RTD from the equation of the parabolic velocity

There exists in CFD two ways to realize a numerical RTD. In the case of a continuous flow, it is necessary to

initially calculate the velocity field of the flow. Then, two options are available:

- Defining a tracer (passive scalar) having the same properties as the fluid flow in an injection input through the boundary conditions and to monitor the concentration of the pseudo-compound to the output. This method requires solving the transient tracer transport that is very time consuming.
- Define solid particles having the same density as the fluid flow and a very small diameter, to inject a quantity large enough to give statistically significant results and observe the time required for each particle to leave the field. The amount of particles that must be injected depends on the accuracy that can be obtained [19].

The distribution of residence time is deduced from the analysis of a large number of paths of the particles in the reactor. This approach has been the subject of fewer studies [20].

This study is based on the calculation of the error between the distribution function of the theoretical residence time for laminar flow equation 6 and the numerical model. The error is calculated by the sum of squared differences. We consider that the flow is fully developed, knowing the analytical solution of Poiseuille flow equation 3 and the traversed distance L. As part of a Lagrangian representation and using the definition of the velocity, which is the derivative of distance with respect to time, we can find the trajectory of point A, by integrating the velocity between 0 and t, we calculated the residence time at each position in our geometry. We have developed three methods of paving to find the coordinates of each position in our geometry inlet. Because of symmetry of Poiseuille flow, we chose a circular paving, then we think for complex geometries where the flows are not necessarily symmetrical so we perform random paving and to enrich our study we achieve a classical paving quadtree (Fig. 1):

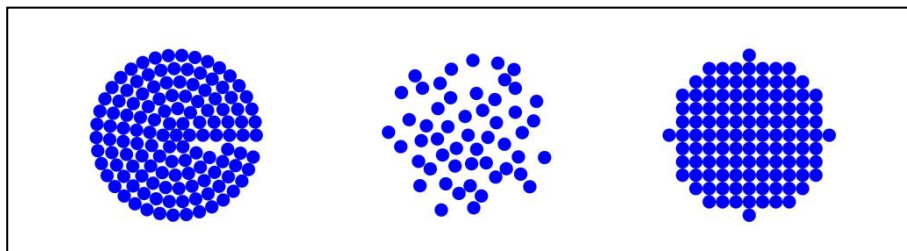


Figure 1 : Paving of the inlet surface (A) circular (B) random (C) quadtree

According to the definition of the distribution function of residence time, we can write equation (1), as a result:

$$E(t) = \frac{C_s(t)}{\int_0^{+\infty} C_s(t) dt} \quad (10)$$

$C_s(t)$ is the fraction of outgoing flow rate between t and $t + dt$ with tracer molecules, the curve $C_s(t)$ represents the curve (RTD) figure 1, standardized in the curve that defines the surface is obtained $E(t)$. To find C_s we get the number of points that lie in the time interval $[t_i, t_{i+1}]$, each point at its own information (transit time, speed and throughput):

$$C_s[t_i, t_{i+1}] = \frac{\sum q_i[t_i, t_{i+1}]}{\sum q_{i \text{ total}}} \quad (11)$$

and are the flow rate of flow tube and the sum of all the flows of current tube there into the inlet surface, respectively. We can write equation 9, as a result:

$$C_s[t_i, t_{i+1}] = \frac{C_s[t_i, t_{i+1}]}{\sum_{i=0}^i C_s[t_i, t_{i+1}][t_{i+1} - t_i]} \quad (12)$$

We assume that around a point in a radius, the fluid moves at the same speed consequently, we have current tubes see Fig. 2. Each point will give a residence time depending on its position in the pipe. As in the Poiseuille flow the velocities near the wall are zero, therefore the residence time associate is long. We will have a variety of residence times, reason for which a statistical study was realized to trace the distribution of residence times.

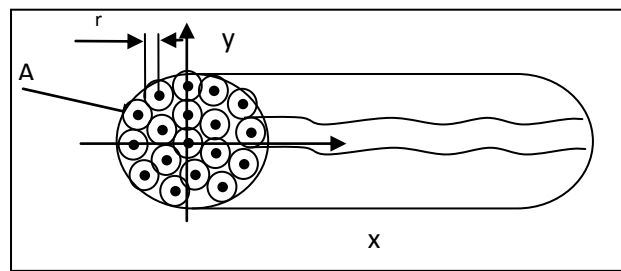


Figure 2 : Flow tubes

2. Results and analysis

Fig. 3 shows the result of the model of residence time distribution. Firstly we use a circular paving; it is adequacy along with the theory with an error of 8%. Secondly the result of the random paving is not in the height because the error is 18% and more costly in computation time, see Fig. 3. Finally 6% of error for the results of quadtree paving is much better compared to circular and random paving and quicker in terms of computation time. Much closer to our numerical model theory, it is best to stay on a quadtree paving.

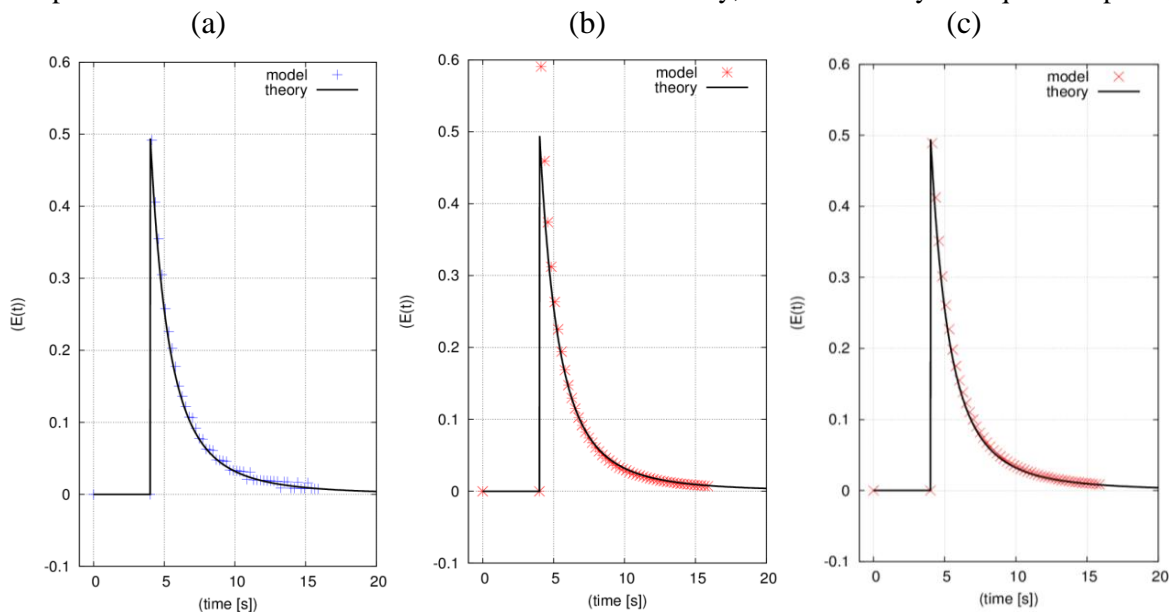


Figure 3 : Model and theory of the distribution function of the residence time for (A) circular (B) random (C) quadtree

3. Prospect

In the next section of this study, we use a velocity field from a numerical simulation of computational fluid dynamics (CFD) instead of the parabolic equation that governs the analytical solution of Poiseuille flow. Then we calibrate the results of the numerical model based on (CFD) with the experimental results.

3.1 Computational Fluid Dynamics (CFD)

Fluid Dynamics is the study of fluids in motion. The basic equations governing fluid motion have been known for more than 150 years and are called the Navier-Stokes equations which govern the motion of a viscous, heat conducting fluid. Various simplifications of these equations exist depending on which effects are insignificant. There are several dimensionless parameters which characterize the relative importance of various effects. Some of these are Mach number, Reynolds number and Prandtl number. Their numerical solution requires the use of the finite volume method; the latter is located in all the codes in general fluid mechanics.

In our study, we use software that is Code_Saturne generalist Computational Fluid Dynamics (CFD) developed by EDF. It allows us to model both compressible and incompressible flows, with or without heat transfer and

turbulence. Like most CFD codes, it requires for meshing and visualization; we used the platform as Salome developed by EDF.

Geoffrey [18] validated the software Code_Saturne a three-dimensional study of gas-solid flow by showing that it can reproduce satisfactorily the axial profiles of pressure gradients.

3.1.1 Navier-Stokes Equation

The continuity equation (conservation of mass):

$$\frac{D\rho}{Dt} + \rho \nabla \cdot \vec{u} = 0 \quad (13)$$

The motion equation (conservation of momentum):

$$\rho \frac{D\vec{u}}{Dt} = -\nabla P - \nabla \cdot \tau + \rho \vec{g} \quad (14)$$

Shear stress constitutive equation:

$$\tau = -\mu \left(\nabla \mathbf{u} + \nabla \vec{u}^T - \frac{2}{3} \nabla \vec{u} \right) \quad (15)$$

The simplified motion equation for an incompressible Newtonian fluid with uniform viscosity

$$\rho \frac{D\vec{u}}{Dt} = -\nabla P - \mu \nabla^2 \vec{u} + \rho \vec{g} \quad (16)$$

3.1.2 Operating conditions

An example was realized with a reactor of internal diameter $D = 0.098$ m and length $L = 4$ m, upstream, there is a venturi in order to ensure the air-helium. This will also work for the injection of particles in the next experiments (gas-solid). Downstream of the reactor, we have a narrowing of the diameter to mix the flow. The geometry and mesh were made by Salome 6.

We performed a numerical simulation of air flow at 20 °C of density of $\rho = 1.29$ kg. m⁻³ and dynamic viscosity $\mu = 1.85 \cdot 10^{-5}$ Pa. In our reactor, the volume flow is 0.00101 m³s⁻¹ to ensure a laminar flow in the reactor with a Reynolds number equal 833.

We have adopted a three-dimensional tetrahedral mesh contains about 6.4×10^5 elements and about 1.5×10^5 nodes with a mesh density of 0.0075 (Fig. 4).

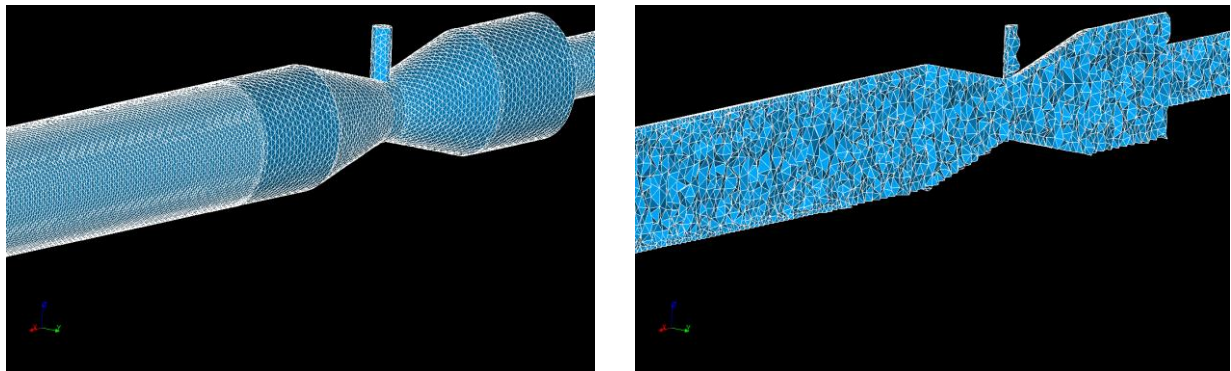


Figure 4 : Mesh of the reactor

The boundary conditions for this calculation CFD, we impose a velocity at the reactor inlet equal to 0.55 m. s⁻¹, a condition of adhesion to the walls which is at zero velocity and atmospheric pressure at the reactor outlet. We have shown in the figures following the velocity profile, and its convergence curve.

Fig. 5 shows the results obtained by CFD, we have a parabolic velocity profile which reflects the presence of a laminar flow in our reactor. We can now replace equation 3, of the previous study, by the current profile.

3.2 Model RTD from a velocity field of CFD

CFD results are contained in a file type MED (Model Data Exchange) which is different depending on the version of Saturn (MED 2.3 and 3.0). The first part of the work was therefore focused on developing an interface compatible with both versions, to extract the necessary information such as number of nodes Fig. 6, elements, node coordinates, the connectivity table of the elements (element-node relation), velocity, pressures ...

As a simulation of finite volume, it should be noted that pressures are at the center of the mesh elements. From the results of the CFD, we propose a simple model based on the kinematics to obtain the trajectory of a particle and this residence time.

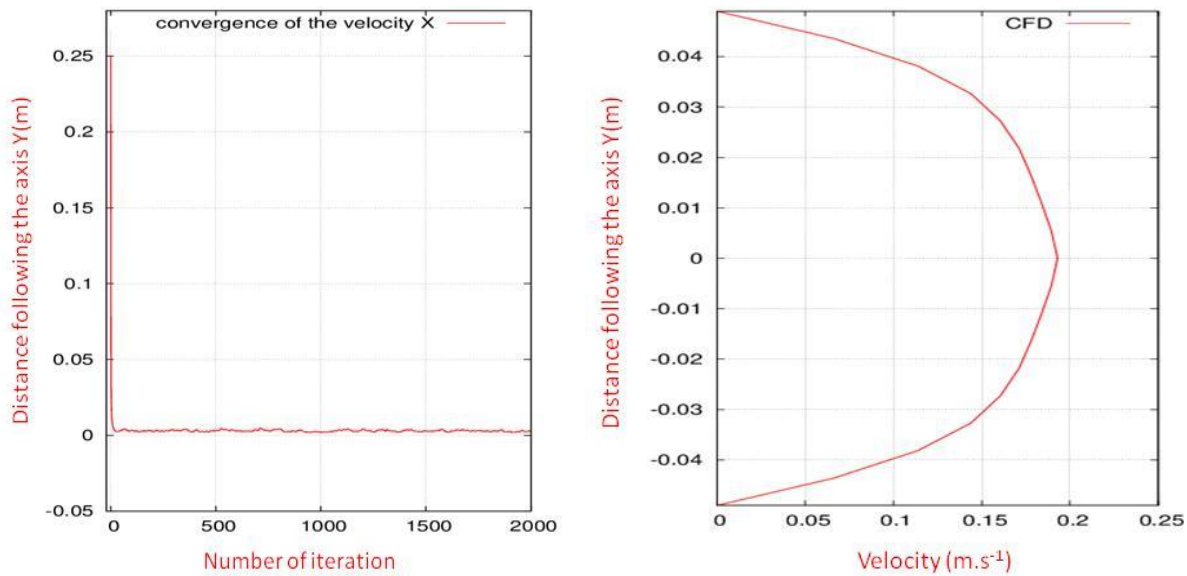


Figure 5 : convergence curve and the profile of the velocity X

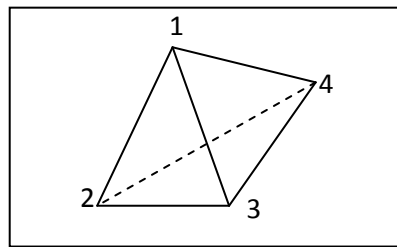


Figure 6 : Tetrahedron, with 4 nodes

As part of a Lagrangian representation, from the definition of the velocity $V(A,t)$ of the particle A:

$$\overrightarrow{V(A,t)} = \frac{d\overrightarrow{A_{(0)}A_{(t)}}}{dt} \quad (17)$$

where (A_0) is the initial position, one can determine its position at any time t by integration:

$$\overrightarrow{A_{(0)}A_{(t)}} = \int_0^t \overrightarrow{V(A,\tau)} d\tau \quad (18)$$

From a numerical point of view, we will estimate the position of A by choosing a regular time steps Δt and estimating the integral previous:

$$\overrightarrow{A_{(0)}A(\Delta t)} = \overrightarrow{A_{(0)}A_{(1)}} = \overrightarrow{V_{(A_0)}} \Delta t \quad (19)$$

Where $\overrightarrow{V_{(A_0)}}$ is the estimated velocity. From the position A_0 , at the moment Δt , we estimate the velocity $\overrightarrow{V_{(A_1)}}$ and recursively find the trajectory of the particle A:

$$\overrightarrow{A_{(k)}A_{(k+1)}} = \overrightarrow{V_{(A_k)}} \Delta t \quad (20)$$

The algorithm stops when the horizontal position of the particle exceeds the length L of the reactor. Using the latest velocity, the residence time T equal to N times Δt

$$T = N \cdot \Delta t \quad (21)$$

where N is the number of iterations

In order to calculate the velocity at any point in the space of our field studies, we use the basic functions of finite elements. Knowing the velocity of the mesh nodes, we can estimate the velocity of the point, in the case of 4 nodes tetrahedron:

$$\vec{V}(A_k) = \sum_{j=1}^4 \vec{V}_j \cdot \varphi(A_k) \quad (22)$$

Where φ the basic functions are defined by the tetrahedron

$$\varphi_j(i) = \delta_{ij} \quad (23)$$

The remaining problem consists of determining which mesh element is the point. To minimize computation time, the grid containing hundreds of thousands of elements, we use a search algorithm $O(n \log(n))$ in order to find the nearest node from the point A_k . Then, from the connectivity table conversely, determine amongst tetrahedron connected to this node, one containing A_k [2].

4. Experimental study

4.1 Experimental determination of the (RTD) by method of tracing Method

The RTD experiments, single-phase flow has been realized in laminar flow on the installation are shown below, so that we can compare the results between numerical and experimental studies, given that we kept the same conditions of operation, mentioned above in the numerical study. A quantity of helium was injected during 80 s which gives us an initial concentration C_0 , the amount of tracer is negligible compared to the volume flow rate of air. At one time we operate a sudden stop of helium using a solenoid valve that allows us to perform a purge signal level.

$$E(t) = \frac{-1}{C_0} \frac{dC_e}{dt} \quad (24)$$

The detection of tracer at the exit of the experimental device is realized by a mass spectrometer, which reflects the concentration of helium in the air or the ratio (Helium/Air) to a signal, which we call the output signal.

We have a gross output signal, which represents the change in the concentration of the tracer as a function of time in the reactor and the line is in fact at the detection of the mass spectrometer, rather than to the output of the reactor. In other words, the output signal that has not the desired signal requires a signal processing by mathematical deconvolution (Fig. 7).

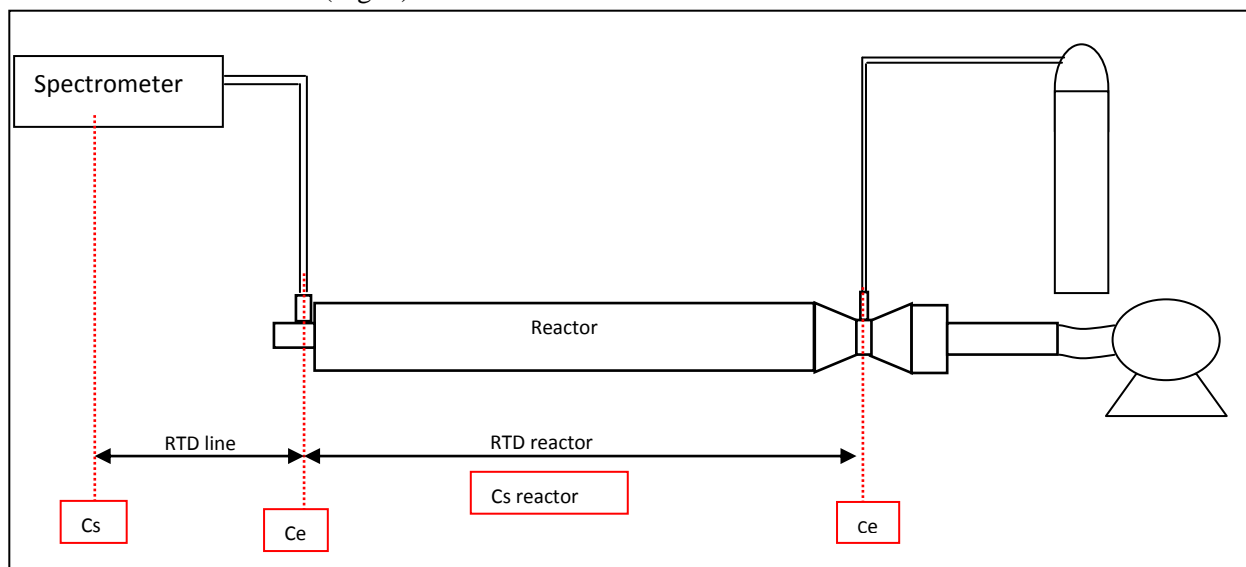


Figure 7 : The principle of deconvolution shown schematically the installation for determining the RTD gas flow

It is assumed that the signal obtained during experimental determination (RTD line + reactor), C_s is the convolution of the signal in the reactor by the distribution function of the residence time of the line, $E(\tau)$

$$C_s(t) = E(\tau) * C_e(t) \quad (25)$$

$E(\tau)$ is the distribution of residence time in the line, the study has been realized only on the line, without the reactor, we vary the air flow rate to model $E(\tau)$ by a function, equal to zero at the plateau (initial concentration C_0) then it decreases exponentially as a result:

$$E(\tau)d\tau = A \exp^{-A\tau} \quad (26)$$

In order to find the coefficient "A" of the equation 26 and generalize the model (Fig. 8), we performed several tests on the experimental set. We note that the variation of the flow rate of the air does not affect the coefficient "A". We can say that whatever the rate of the distribution of residence time in line, is the same as $A = 0.85$ was not too far from finding coefficient by Mahmoudi. In these research works he found $A = 1.08$ [18].

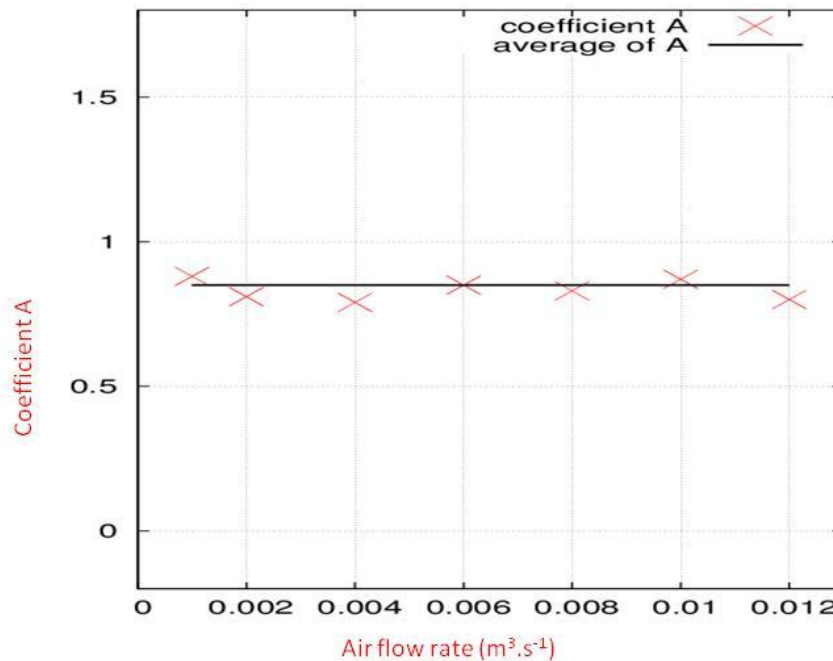


Figure 8 : coefficient "A" as a function of volume flow of the air

Once the $E(\tau)$ determined, we can access the deconvolution by the reconstitution of the signal of C_e . we can write equation 25 as a result

$$C_s(t) = \int_0^{\infty} C_e(t-\tau) \cdot E(\tau) d\tau \quad (27)$$

Knowing that convolution operator corresponds to a summation with a phase shift. In practice, it is necessary to discretized the input function ($C_e(t)$) and (RTD): $E(\tau)$ then add each segment taking into account the phase shift

$$C_s(t) = \int_0^{\tau_1} C_e(t-\tau) \cdot E(\tau) d\tau + \int_{\tau_1}^{\tau_1+\Delta\tau_1} C_e(t-\tau) \cdot E(\tau) d\tau + \int_{\tau_1+\Delta\tau_1}^{\infty} C_e(t-\tau) \cdot E(\tau) d\tau \quad (28)$$

$$C_s(t-\tau_1+\Delta\tau_1) = \frac{C_s(t_1-\tau_1) - C_e(t_1-\tau_1) \exp(-A\Delta\tau_1)}{E(\tau_1)\Delta\tau_1} \quad (29)$$

This resolution was realized in a numerical iterative manner. The signal is reconstructed so we have represented on the figure below an example of the concentration signal collected at the spectrometer and determined at the reactor outlet. We can see through an offset between the two signals is of the order of 20 seconds which represents the residence time of the first molecule of the tracer (helium), detected by the mass spectrometer.

C_s denotes the overall signal, In other words the signal measured by the mass spectrometer. C_e is the reconstructed signal by the method of mathematical deconvolution. By equation 24, we obtain the mean residence time:

$$\bar{t}_s = \int_0^{\infty} t E(t) dt \quad (30)$$

5. Comparison of numerical and experimental results

In order to compare the experimental test results with the numerical model of the (RTD), we chose to present the results of numerical distribution of residence time found with the method of quadtree paving which gives the best results.

Figure 9 show that the residence time distribution of the numerical model is equal 26.31 s and the experimental is equal to 26.64 s. The model that is developed appears to be a good descriptor of the average residence time of the experimental study with the minor error between them approximately 1%.

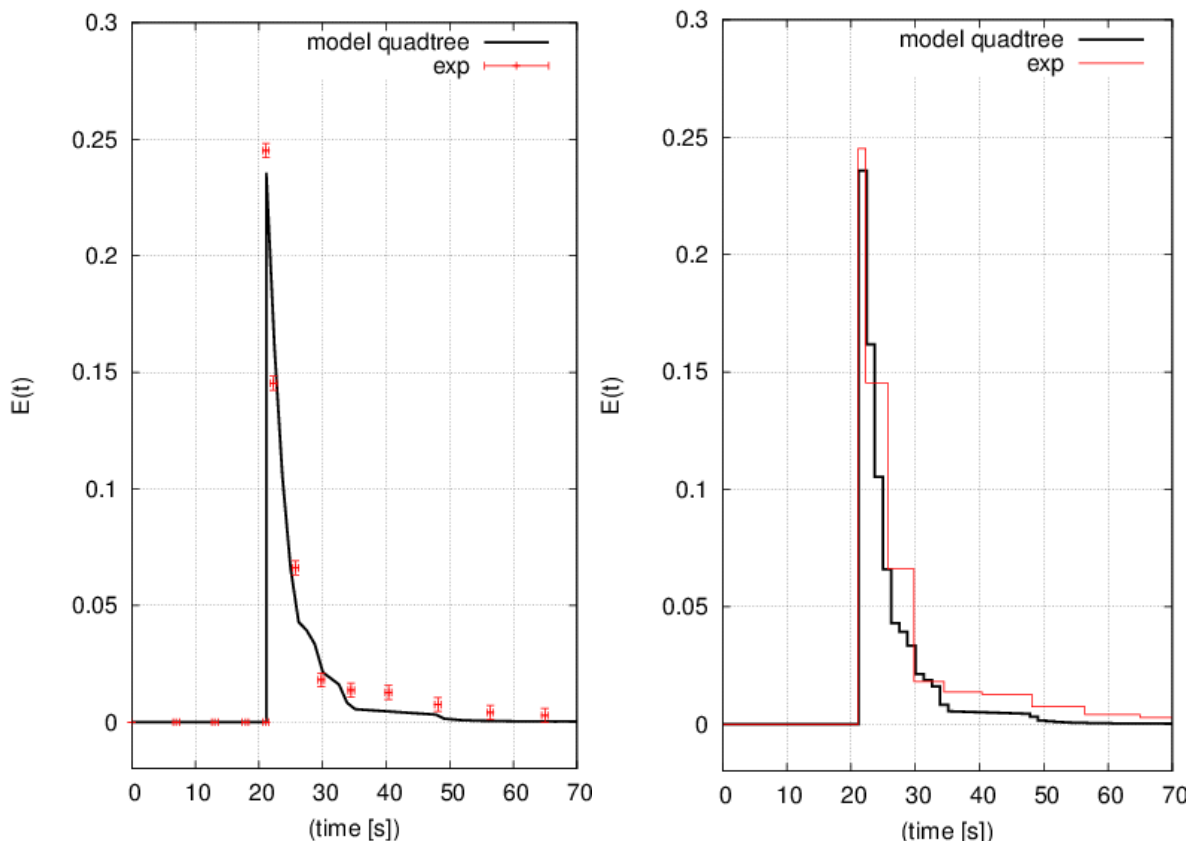


Figure 9 : the comparison between experimental and numerical model RTD with paving quadtree

Conclusions

The RTD method has been widely applied in industrial continuous flow systems. It offers a convenient tool for understanding material transport phenomena inside various unit operations, which is the first step for efficient operation design, troubleshooting, and system improvement. An alternative of the predictive modeling is the application of CFD or DEM simulations, where validation and verification of the simulations with experimental results is always required.

The development of the inline tracer detection method, especially for solid systems, is also a promising direction that requires additional work. Regarding the interests of the numerical model developed in this study. This last are very important because we get the full trajectory each particle and her residence time the higher the resolution of transport equations by CFD, the ease with which we can adjust the accuracy of the simulation, by choosing a number of paving stones more or less. In our case it is the order of one hundred miles. Ultimately if the objective of the study is an Operating residence time distribution, the particle tracking method is ideally suited.

In subsequent studies, we will launch to the two-phase gas-solid flows, to couple the dynamics (CFD) and (DEM) to expand our numerical model actual and make it applicable to the determination of the residence time distribution for two-phase flows. Then we will calibrate the results of the numerical model based on (CFD and DEM) with the experimental results.

Acknowledgements - This work was performed within the Picardie region funded by the European Commission.

References

1. Harris A.T., Thorpe R.B., Davidson J.F., *J. Chem. Eng.* 89 (2002) 127-142.
2. Coorevits P., Marie C., Benhabib K., *Europ. J. Comp. Mec.* 20 (2011) 487-502 .
3. Dankwert P.V., *Chem. Eng. Sci.* (1953) 1–13.
4. Nauman E.B., *Ind. Eng. Chem.* 12 (2008) 3752–3766.
5. Agar D.W., *J. Chem. Eng.* 21 (2008) 431–438.
6. H. Christian, *Chem. Eng. Sci.* 12 (2009) 64.
7. Desjardins A., *mémoire de maitrise sciences appliquée, Canada.* 1999.
8. Wein O. U., Ulbrecht J., *Chem. Com.* 36 (1972) 3240–3259.
9. Wein O., Ulbrecht J., *Chem. Com.* 16 (1972) 3240–3259.
10. Ziegler G.R., Aguilar C.A., *J. Food. Eng.* 18 (2003) 161–167.
11. Trachsel F., Günther A., Khan S., Jensen K.F., *Chem. Eng. Sci.* 15 (2005) 5729–5737.
12. Cantu-Perez A., Bi S., Barrass S., Wood M., Gavriilidis A., *Appl. Therm. Eng.* 10 (2011) 634–639.
13. Rodríguez-Rojo S., López-Valdezate N., Cocero M.J., *J. Supercrit. Flui.* 6 (2008) 433–440.
14. Nikitine C., Rodier E., Sauceau M., Fages J., *Chem. Eng. Res. Des.* 87 (2009) 809–816.
15. Baron R., Vauchel P., Kaas R., Arhaliass A., Legrand J., *Chem. Eng. Sci.* 38 (2010) 3313–3321.
16. Vanarase A.U., Muzzio F.J., *Powder Tech.* 34 (2011) 26–36.
17. Diep J., Kiel D., St-Pierre J., Wong A., *Chem. Eng. Sci.* 2007. 846–857.
18. Geoffrey P., Thesis, *Toulouse*, 2005,.
19. Mahmoudi S., Seville J.P.K., Baeyens J., *Powder Tech.* 54 (2010) 322–330.
20. Gao Y., Vanarase A., Muzzio F., Ierapetritou M., *Chem. Eng. Sci.* 85 (2011) 417–425.

(2015) ; <http://www.jmaterenvironsci.com>